How Finite Element Analysis Revolutionized a 100-Year Old Equation

Arle JE[1,2,3], Shils JL[4], Mei L[1], and Carlson KW*[1]

[1]Department of Neurosurgery, Beth Israel Deaconess Medical Center, Boston, MA, USA
[2]Department of Neurosurgery, Harvard Medical School, Boston, MA,, USA
[3]Department of Neurosurgery, Mount Auburn Hospital, Cambridge, MA, USA
[4]Department of Anesthesiology, Rush Medical Center, Chicago, IL, USA
*Corresponding author: Mount Auburn Hospital, 300 Mount Auburn St., Cambridge, MA 02138.
kwcarlso@bidmc.harvard.edu

Abstract: In 1901 Weiss proposed an equation predicting activation of nerve fibers by electrical stimulation, used for a century in neuroscience and 30 years in neuromodulation, which applies electric fields to modify nerve behavior in neurological disorders. Since it is difficult to measure electric potential *along a nerve fiber*, Weiss' equation instead relates voltage or current applied *at the electrode* to action potential thresholds at the nerve, and thus thresholds are relative to the model's geometry, electrode array configuration, tissue conductivities, and waveform.

We replicated a leading calibrated nerve model in COMSOL and with it, examined the predicted electric potential gradient *seen by the axon*. This made it possible to convert a subjective equation predicting nerve thresholds to an absolute equation. We use the new method in our analyses of neuromodulation, e.g. of the spinal cord for chronic pain and vagus nerve for treatment of epilepsy.

Keywords: nerve fiber, axon threshold, neuromodulation, chronic pain, epilepsy.

1. Introduction

1.1. The Weiss equation of nerve fiber activation.

The Weiss equation is a bastion of neuroscience, predicting nerve fiber activation by external electrical stimulation [1]:

$$I_{th} = I_{rh}(1 + \frac{\tau_{ch}}{pw}) \quad (1)$$

where I_{th} is the minimum current required to generate an action potential (AP), I_{rh} is the rheobase current, pw is pulse width (duration of the stimulating pulse), and τ_{ch} is the pulse width when twice the rheobase current is applied to the fiber. Rheobase and chronaxie together determine the *strength-duration curve* for nerve fibers (Sec. 1.2 and Geddes [1]).

Weiss' original equation and variations of it have been used for over a century in neuroscience and in the last two decades in neuromodulation, the set of protocols applying electromagnetic fields to modulate neural circuits in humans. Neuromodulation became one of medicine's fastest-growing fields because it works on patients whose conditions are drug-resistant. Now organizations such as DARPA and SmithKline Glaxo have 'electroceutical' initiatives to find stimulation protocols for the entire human nervous system. Consequently, the Weiss equation has become increasingly important in neuroscience.

1.2. Nerve fiber strength-duration curves.

In Fig. 1, the y-axis of the graph shows the stimulation amplitude, which can be voltage or current, emitted at the electrode. Then the firing threshold of the nerve fiber ('axon') is measured with a separate recording electrode. At long pulse widths, less amplitude is required than at short pulse-widths, since the fiber integrates the signal over time, minus a small leak current (the 'leaky capacitor model'), and the amplitude required if the pulse width is infinite (in practice ~ 2 ms), i.e. the lowest amplitude that will fire the axon, is its *rheobase*. The rheobase is not zero since it must exceed the leak current in order for there to be net charge accumulating at the axon over time.

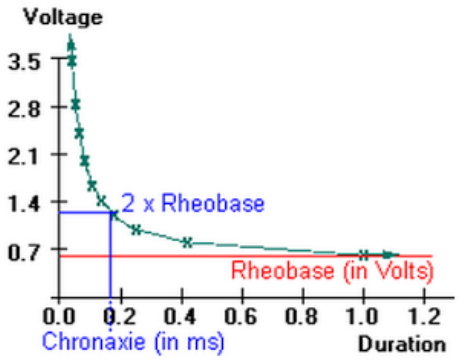

Figure 1. A generic *relative* strength-duration plot of a nerve fiber described by the Weiss equation. The plot is relative to the geometry, conductivities, electrode array, and waveforms of a particular application.

The pulse width that will fire the axon at twice the rheobase amplitude is its *chronaxie*, which is the corner point of the strength-duration curve and the point of minimum energy required to fire the axon [1]. It is the *gradient* of potential along the axon, called its 'activating function' (AF), which triggers it to fire an action potential [2]. Axons can be without any fatty myelin insulation, or myelinated to varying degrees, with myelin 'beaded' along the axon and separated by gaps called nodes of Ranvier. Thicker, more myelinated axons also have longer internodes between the nodes of Ranvier, which means the electric potential gradient and AF, measured as the 2nd difference between the nodes, is steeper for them than for thinner axons. Consequently, the thicker the axon, the lower is its threshold [3].

The amplitude used in the Weiss equation and strength-duration curves has always been measured at the electrode emitting the signal. Stimulus amplitude actually reaching the axon is unknown and difficult to measure *in vivo* [4]. Therefore strength-duration curves were always relative, not absolute, since the amplitude required at the electrode to stimulate the axon was subject to geometry (e.g. the separation between electrode and fiber), material conductivities, the configuration of electrodes if an array were used, and waveform.

2. Methods and Use of COMSOL Multiphysics® Software

2.1. Theoretical basis; implementation

Finite element modeling (FEM) permits one to examine the microcosm of the axon and predict quantities at individual nodes of Ranvier such as field potential, field potential gradient, AF, and current density, a proxy for accumulated charge. In particular the AF may be substituted for electrode amplitude as the rheobase quantity to calculate fiber threshold strength-duration curves, thus creating an absolute, not relative, rheobase, as an independent variable in a modified Weiss equation.

Thus the rheobase formula we use is based on FEM measurements of fiber thresholds in our COMSOL replica of the Wesselink et al. fiber threshold model (Fig. 2), which was calibrated to human fiber qualities [5-7]. Governing equations are those of the AC-DC module for electrostatics, and geometrical parameters, conductivities, mesh validation, etc. are discussed in Arle et al. [5]. Thresholds are then predicted using the AF on axons in our spinal cord stimulation (SCS), vagus nerve stimulation (SCS), and other FEMs.

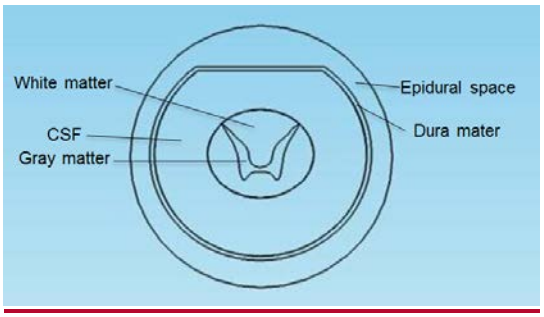

Figure 2. 2D geometry slice of a 3D COMSOL model of the spinal cord used to calibrate an absolute version of the Weiss equation used to predict fiber thresholds. Epidural space: ambient medium (grounded). Dura mater: tough, resistive covering of the spinal cord. CSF: conductive cerebrospinal fluid. White matter: nerve fibers encased in whitish, fatty insulation (myelin) that transmit signals from peripheral receptors to neurons in the spinal cord and to and from the brain and spinal cord. Gray matter: Neurons.

One can include a factor for fiber diameter in the rheobase formula in order to calculate predicted thresholds for fibers of different diameters via the Weiss formula (1). Here the constants are from our SCS model using a

sample length of 0.5 mm along the axon to calculate 2nd differences in the AF [5]:

$$V_{rh} = 0.0019 + 0.0183\, e^{-diam/4.55} \quad (2)$$

$$\tau_{ch} = 119.00 + 268.44\, e^{-diam/4.14} \quad (3)$$

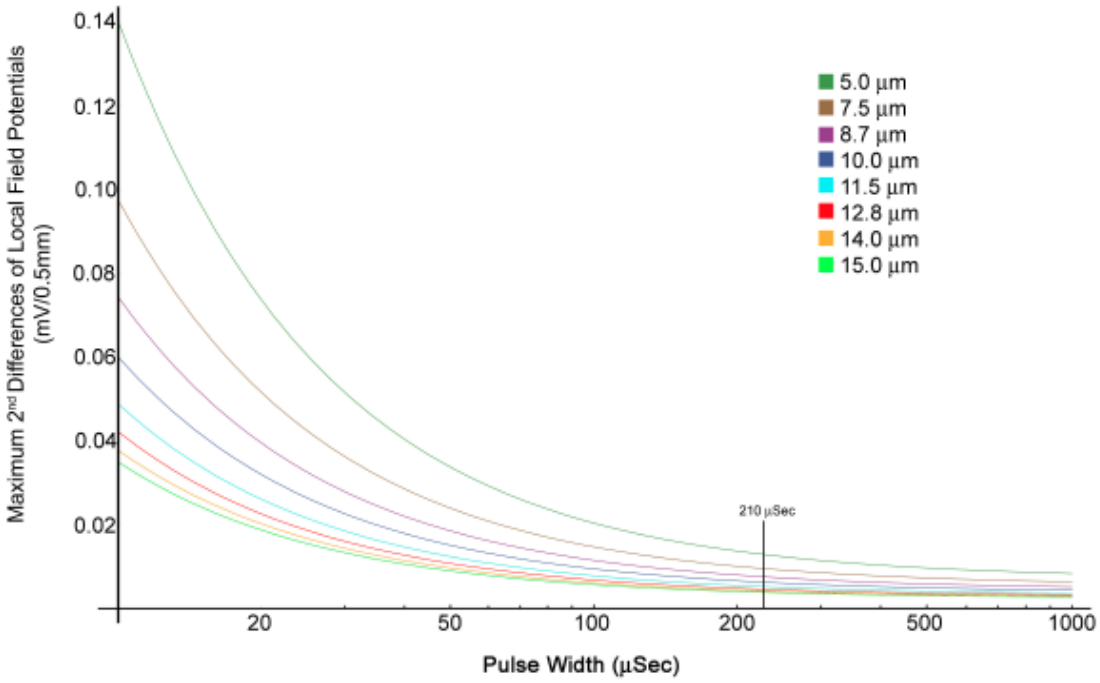

Figure 3. An *absolute* strength-duration plot of different diameter nerve fibers (legend) calculated from the Weiss equation in which 2nd differences of electric potential along the axons (y-axis), as predicted in a COMSOL FEM, are substituted for potential measured at the electrode, the traditional method. X-axis: duration of stimulating pulse.

2.2. Key limitations

In this method, chronaxie remains subject to the five factors described by Geddes [1]. In VNS, for example the key factors are the conductivities of the inhomogeneous vagus components and the varying distance of the fibers from the electrodes. Thus, the same diameter fiber will have differing chronaxies depending on its location in the nerve.

Secondly, while the model has been validated for configurations in which nerve fibers are vertically oriented and distal to the stimulating electrode (e.g. > 0.5 mm), it has not been validated for nerve fibers proximate to the electrode, for instance, in deep brain stimulation.

2.3. Model Validation

The chronaxie calculated for a fiber at a single location by Wesselink et al. in a model of SCS [6] compared favorably with VNS estimates in dog [8-10], pig [11] and human [12].

In a model of SCS based on clinical data from human patients, Lee et al. investigated fiber activation using a different electrode configuration (a percutaneous electrode lead) and correlated fiber thresholds from a different fiber model, the McIntyre-Warman-Grill active fiber model [13] with their data [14]. While tissue conductivities were similar to those in the Holsheimer model, the geometry of the Lee

model, notably the cerebrospinal fluid thickness, which is a key variable between individual patients, spinal cord dimensions, ambient medium structure and grounding method, and method of activation of the fibers using a percutaneous cylindrical 'guarded tripole' array (two anodes flanking the single cathode) versus square monopole electrode, were different. As a check on our absolute model's accuracy, we built a replica FEM of the Lee et al. model in COMSOL and found the maximum AF in our model for 8.7 and 11.5 µm fibers were within 10% of its predicted values.

3. Results

Two examples of model application are SCS and VNS, but in principle the absolute threshold formula can be used in many neuromodulation applications.

3.1 Effect of scar formation in spinal cord stimulation

SCS via a reversible surgical procedure is highly effective in reducing pain in patients for whom other measures (e.g. physical therapy, drugs, and other surgical procedures such as fusion) have failed.

We used the initial model to examine the manner in which inexorable formation of electrically resistive, fibrotic scar tissue under an electrode array implanted on the spinal cord affects electric field distribution in the white matter (nerve fibers) of the cord [5]. The geometry was created in SolidWorks (Waltham, MA) and imported into COMSOL via LiveLink (Fig. 4).

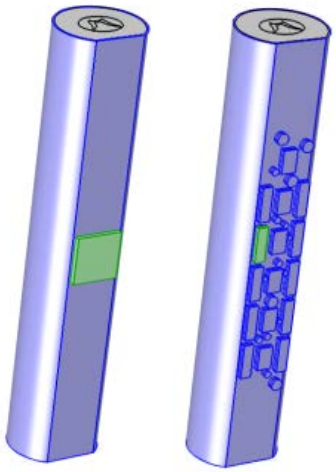

Figure 4. FEMs of the spinal cord. Left: Model using a single electrode (monopole, green) to replicate a model of nerve fiber activation calibrated to human parameters by Wesselink et al. [6]. Right: Model using an electrode array typically applied to treat chronic pain in spinal cord stimulation. Electrodes are often activated transversely (e.g. green electrode) or longitudinally, flanking a central cathode, to contain the field of the cathode. Small circles are simulated pieces of electrically resistive scar, which is also modeled in 3 layers under each electrode. Thus a very large number of combination of scar tissue and electrode activation can be modeled to examine the complex effects of electrode array and scarring.

Counter-intuitively, in a guarded tripole of similar electrode configuration where anodes flank a cathode with design intent of focusing and containing the cathodic field, we found that resistive scar under any anode 'unleashes' the cathodic field, *increasing* the overall number of nerve fibers activated, and inadvertently can cause side effects and loss of pain relief (analgesia) in the targeted regions (dermatomes) (Fig. 5).

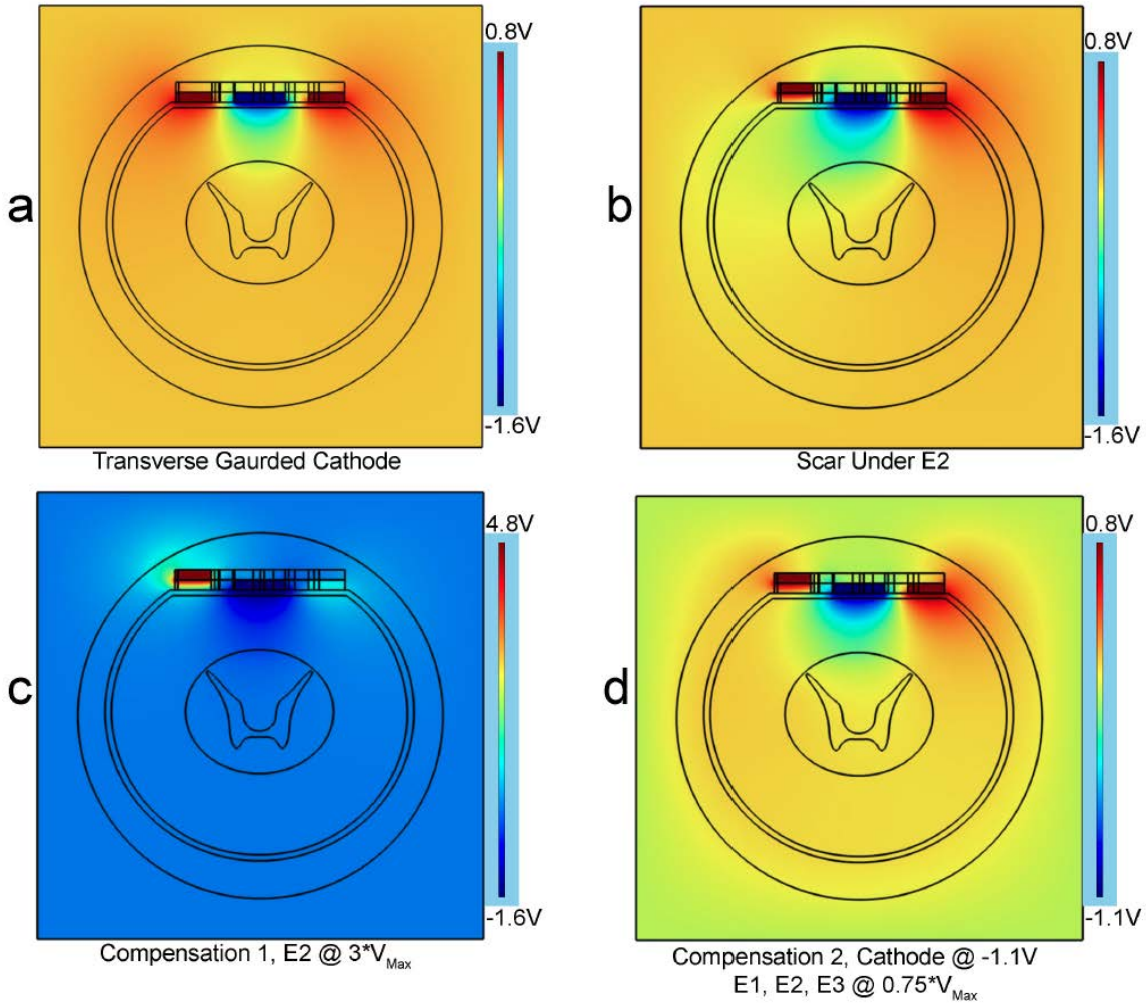

Figure 5. Examination of the electric field in spinal cord stimulation, pre- and post-scar formation (COMSOL slice plots). a: Cathode is flanked laterally by two anodes. Field generated by this configuration is as intended with cathodal field penetrating the superficial central portion of the white matter (nerve fibers, center ellipse) in the spinal cord, resulting in pain relief (analgesia). b: Scar under the left anode causes the cathodal field to expand and drift left, causing large numbers of untargeted fibers to be activated, resulting in side effects and loss of analgesia. c: A failed attempt to increase the electrode stimulation amplitude above the scar tissue to compensate for the loss of anodal field strength by the anode. d: A partially successful attempt to add anodes above and below the anode affected by scar tissue to compensate for its effective amplitude reduction by the scar.

3.2 Examination of the nerve fibers implicated in vagus nerve stimulation.

VNS is effective in about 60% of patients for whom drugs have failed to reduce seizure frequency. The reasons why it is not effective in all patients are unknown.

We used the absolute fiber model and extended it to include nerve fiber *blocking* to examine intended and inadvertent nerve fiber activation and blocking in VNS [7]. A blocking factor of 5.5x the fiber activation threshold was determined from blocking studies in the literature and trials with our active fiber model across fiber diameters 2 – 15 µm. This model used geometry built with native COMSOL CAD tools and meshed and solved far faster than with geometry imported from an external CAD program. Consequently we were able to run long time-dependent simulations and parameterize many dependent variables, permitting parameter sweeps that allowed examination of those

variables with wide error bars or variance across patients (e.g. nerve thickness). See Arle et al. [7] for detailed model parameter specification and use of the AC-DC module electrostatics physics.

In VNS to date, flexible helical electrodes are used, which minimize trauma to the nerve on implantation. A key finding of our study was that with typical nerve diameters of 2 – 4 mm, partial encirclement of the nerve by the electrodes results in a gap of nerve activation, which is more pronounced in the superficial region (Figs. 6 & 7). Since there is evidence that fibers responsible for efficacy and side effects (hoarseness) are located superficially within the nerve, the existence of the gap implies a lack of control over efficacy and side effects in perhaps ¼ of the patients (if the average gap is 25% of nerve circumference), possibly helping to explain responder rates that are considerably less than 100%.

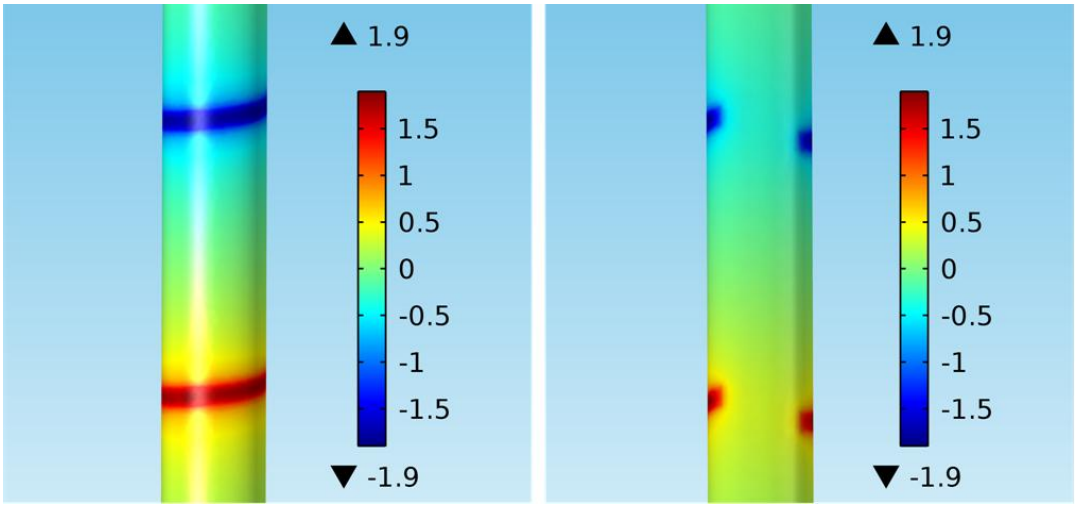

Figure 6. Volume plots of electric potential (V) from the COMSOL model of helical electrodes (cathode, top; anode, bottom) partially encircling the vagus nerve used to treat epilepsy showing adequate coverage of the nerve (left) but also a gap in coverage (right). If fibers responsible for efficacy and side effects are located superficially, for which there is evidence, the gap produced by this configuration will result in inadvertent lack of efficacy and production of side effects.

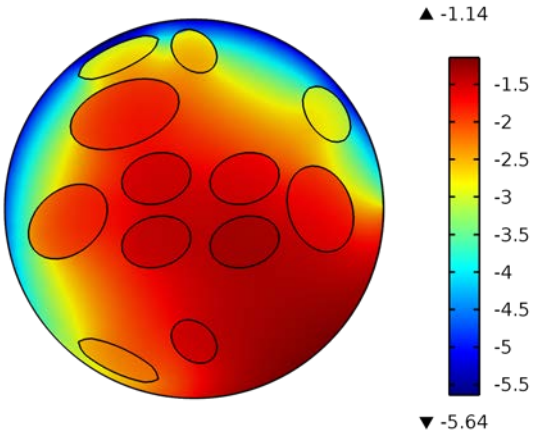

Figure 5. Slice plot of electric potential (V) under the cathode in the vagus nerve showing gap in uniform field penetration due to partial encirclement by helical electrodes. Ellipses are bundles of nerve fibers (fascicles), which are enclosed in electrically resistive tissue (perineurium). The perineurium and 110 µm of scar tissue surrounding the nerve were modeled via thin layers and contact impedance, respectively, programmatically implemented in COMSOL rather than through geomettry, a technique which significantly reduces mesh issues, and mesh and solve time.

4. Conclusions

FEM can examine the microcosm of the axon and the electric field along its surface. FEM thus renders a physical quantity that was previously unobservable, observable, like Galileo's observation of the surface of the moon with a

telescope, or van Leuwenhoek's observation of microbes with a microscope.

Using COMSOL, we measured what is known as the 'activating function' of the fiber and used that value instead of the electrode amplitude as the rheobase quantity in the Weiss equation. Thus we created absolute, rather than relative, fiber strength-duration curves (Fig 3). We corroborated our theoretical model against clinical data for 8.7 and 11.5 µm fibers and its predictions were within 10% of empirical values.

5. References

1. Geddes LA. Accuracy limitations of chronaxie values. *IEEE Trans Biomed Eng*, **51**, 176-181 (2004).
2. Rattay F. Analysis of models for external stimulation of axons. *IEEE Trans Biomed Eng*, **33**, 974-977 (1986).
3. Molnar G, Barolat G. Principles of cord activation during spinal cord stimulation. *Neuromodulation*, **17 Suppl 1**, 12-21 (2014).
4. Aalbers M, Vles J, Klinkenberg S, Hoogland G, et al. Animal models for vagus nerve stimulation in epilepsy. *Exp Neurol*, **230**, 167-75 (2011).
5. Arle JE, Carlson KW, Mei L, Shils JL. Modeling effects of scar on patterns of dorsal column stimulation. *Neuromodulation*, **17**, 320-333 (2014).
6. Wesselink WA, Holsheimer J, Boom HB. A model of the electrical behaviour of myelinated sensory nerve fibres based on human data. *Med Biol Eng Comput*, **37**, 228-35 (1999).
7. Arle JE, Carlson KW, Mei L. Investigation of mechanisms of vagus nerve stimulation for seizure using finite element modeling. *Epilepsy Res*, **126**, 109-18 (2016).
8. Castoro MA, Yoo PB, Hincapie JG, Hamann JJ, et al. Excitation properties of the right cervical vagus nerve in adult dogs. *Exp Neurol*, **227**, 62-8 (2011).
9. Smith CD, Geddes LA, Bourland JD, Foster KS, et al. The Chronaxie and Propagation Velocity of Canine Cervical Vagus Nerve Fibers In Vivo. *Cardiovascular Engineering*, **1** (2001).
10. Yoo PB, Lubock NB, Hincapie JG, Ruble SB, et al. High-resolution measurement of electrically-evoked vagus nerve activity in the anesthetized dog. *J Neural Eng*, **10**, 026003 (2013).
11. Anholt TA, Ayal S, Goldberg JA. Recruitment and blocking properties of the CardioFit stimulation lead. *J Neural Eng*, **8**, 034004 (2011).
12. Helmers SL, Begnaud J, Cowley A, Corwin HM, et al. Application of a computational model of vagus nerve stimulation. *Acta Neurol Scand*, **126**, 336-43 (2012).
13. McIntyre CC, Richardson AG, Grill WM. Modeling the excitability of mammalian nerve fibers: influence of afterpotentials on the recovery cycle. *J Neurophysiol*, **87**, 995-1006 (2002).
14. Lee D, Bradley K, Kormyio N, Moeller-Bertram T, *Investigation of fibers activated in spinal cord stimulation (SCS) using a computational model*, in *15th North American Neuromodulation Conference*. 2011: Las Vegas NV USA.

6. Acknowledgements

The work contained in this paper was performed under a generous grant from the Sydney Family Trust and funding from Livanova Neuromodulation (then Cyberonics Corp,).